JEE Journal of Ecological Engineering

Journal of Ecological Engineering 2022, 23(9), 115–127
https://doi.org/10.12911/22998993/151746
ISSN 2299–8993, License CC-BY 4.0

Received: 2022.06.17
Accepted: 2022.07.08
Published: 2022.08.01

Optimization of Graphene Oxide Mixed Matrix Membrane for AB-210 Dye Removal

Ammar A. Al-Sultan[1*], Rana J. Kadhim[1], Omar H. Al-Emami[1], Qusay F. Alsalhy[2], Hasan Sh. Majdi[3]

[1] Civil Engineering Department, University of Technology, Alsinaa Str. 52, 10066, Baghdad, Iraq

[2] Membrane Technology Research Unit, Chemical Engineering Department, University of Technology, Alsinaa Str. 52, 10066, Baghdad, Iraq

[3] Al-Mustaqbal University College, 51001, Babylon, Iraq

* Corresponding auhtor's e-mail: ammar.a.alsultan@uotechnology.edu.iq

ABSTRACT

This research aimed to find the best-operating conditions for incorporating the GO material into PES/GO membranes for the NF applications. Organic dye molecules may foul GO-NP/PES membranes. The improved model aimed to reduce the energy lost while maintaining a high system discharge throughout the treatment process in order to face the technical problems that the membranes are exposed to. To create a particular amount of flux above the intended values, an optimization approach was used to find the optimal values for several important parameters in the process. To enhance the process effectiveness on a broader scale, mathematical and statistical studies, such as response surface methodology and statistical analysis of the parameters (ANOVA), were applied. The impact of operational factors, like the pH values of the dye feeding (3–11), GO weight content (0–2 wt.%), dye concentration (10–100 ppm) of AB-210, and the interfaces for these factors with the PES/GO membrane permeability was examined. The PES membrane had the best performance, with a result of 131.2338 $L \cdot m^{-2} \cdot h^{-1} \cdot bar^{-1}$. The pH did not influence the AB-210 dye reaction, and the Pareto chart of the standardized effects on dye permeation flux using statistical comparison at the 5% significance level supports these findings.

Keywords: optimization, nano filtration, membrane, industrial wastewater, graphene oxide**,** dyes.

INTRODUCTION

Due to a lack of freshwater sources and the massive influx of industrial wastewater and sewage, pollutant concentrations in water have increased, and this problem has grown into a major challenge that threatens humanity and life on the planet. The population increase, especially in developing countries, the development of industries, and economic growth call for the necessity to use safe and sustainable technologies to meet this global challenge. Industrial water treatment by separating pollutants and purifying water from them is one of the necessary and complex processes in many industries, such as those of leather, tanning, dyes, petrochemical, and oil refining (Obiad and Al-Sultan 2020). Industrial wastewater treatment represents a major environmental challenge for many engineers to maintain a safe environment on the one hand, and the possibility of reusing the treated water to achieve water sustainability on the other. These molecules may be free-form or combined with other compounds, such as heavy metals, to produce the pollutants that are difficult to treat (Al-Sultan et al. 2019). Permeable media may be used to separate the pollutants from water, as in the case of using sand as a porous medium to remove some dyes and heavy metals. However, this method is not effective in removing particular particles such as dyes. During the past two centuries, the upgrading in the enclosed operations has been rapidly developing using multi lab physical modern techniques, for instance, centrifugation,

distillation and softening, adsorption of moleculers, crystallization, extraction of elements, etc.

The most modern upgrade in the treatment processes is using the membranes, which are used as a semi-permeable baffle that permits the split of pollutants (Sarbatly 2020). There is a variety of membranes based on the characteristics, configuration, setup, and usage. It is difficult to devise a complete description of membranes that encompasses all of their features. Membranes can be made as permeable or non-permeable, symmetrical or asymmetrical, thick or thin, homogeneous or non-homogeneous, semi-liquid or semi-solid, and neutral that may carry positive or negative electrostatic charges (Fauzi and Matsuura 2016, Sarbatly 2020).

Membrane synthesis techniques are primarily sorted depending on their void size and the potential segregation force. The membrane skin thickness is classified within a range of 100 nm – 1 cm, while the membrane void size is made from ≤ 0.1 nm to many micrometers (Judd and Judd 2011). The operation mode of the membrane can be paid by the power loss gradients in a milestone of the applied force over membrane surface area, reverse osmotic pressure, the density of mass, electro-static charge, heat conductivity, or any load combination of the potential applied forces. There are other classifications of membranes except for the above; for example, a membrane represents a combination of the properties like porous media, asymmetrical, and carries an electrostatic charge (Judd and Judd 2011, Park, Chang et al. 2015). The high level of toxicity and pH of dyes are among the popular and significant issues in wastewater (Van der Bruggen et al. 2001, Lin et al. 2016). They represent the primary cause in the coloration of cellulose strings (like cotton). The addition of reacting dyes leads to decisive ecological issues (Koyuncu 2002). These pollutants lead to difficulties in the treatment of wastewater associated with textile manufacturing, which results from dye particles and their resistance to aerobic phase treatment, oxidation, lighting, and heating. Hence, wastewater becomes more complex for treatment (Majewska-Nowak 2009).

The textile industry produces the dyes in the environment, yielding around 50% of the dye effluent wastewater worldwide (De Gisi et al. 2016). Therefore, it is vital to use safe, economic, and effective wastewater purification techniques. Membrane segregation is a modern treatment model for treating dyes. Membrane sorting technology, and its upgrading, represent the optimum way to overcome water shortage by producing the best-quality of freshwater to humans. This technology has distinguished advantages, like low operation cost, high efficiency of pollutant separation, accuracy, simple operation, and more ecological friendliness than traditional wastewater treatment methods. For this reason, the afore-mentioned technology has been used in several industries, like food, pharmaceuticals, dyes, and salty water purification (Moussavi and Mahmoudi 2009, Pendergast and Hoek 2011, Alsalhy et al. 2017, Yaseen and Scholz 2018).

There have been dozens of studies that described the use of hydrophilic materials and particles as nanofillers in combination with polymers to improve the solubility and anti-foul performance of ultrafiltration membranes. Throughout the last ten years, many researchers have focused on using GO-NP as an effective media that is used to separate dyes, due to its remarkable duplicated two-dimensional model of configuration; it has shown a more extraordinary adsorption ability for certain dye molecules (Geim and Novoselov 2007, Geim 2009, Gerken et al. 2009, Jin et al. 2013, Junaidi et al. 2018, Alyarnezhad et al. 2020).

Because of the extraordinary features of the polymer that result from the insertion of GO sheets into it, it is extremely desirable for a variety of applications. These characteristics provide a two-dimensional geometry, the capacity to generate negative electrostatic interactions, exceptional charge transport, large surface area, innocuity, and extraordinary high chemical stability, among others. The texture and mechanical behavior of membranes, as well as the impacts of contamination, may be altered by GO as well. It can keep improving mechanical properties, minimize organic tendency, and efficiently segregate dyes by increasing the water membrane performance and exterior hydrophilicity (Zinadini et al. 2014, Mahmoud et al. 2015).

Several researchers utilized GO as a filler in a series of separation procedures to improve the performance of polymeric membranes and to develop nanocomposite membranes (MMMs) (Zhao et al. 2014, Kumar et al. 2015, Abdel-Karim et al. 2018, Akbari et al. 2018, Gholami and Mahdavi 2018, Makhetha and Moutloali 2018, Wang et al. 2019, Luque-Alled et al. 2020). They verified that GO is a viable choice for supporting membrane water flow and preserving/maintaining a high percentage of waste.

This research aimed to investigate the preparation of MMMs that have a more extraordinary ability to remove substantial toxic dyes from industrial wastewater. Developing a PES membrane to remove high toxic dyes like Acid Black (AB-210), which are soluble in the effluents from tanneries and paper and textile factories, has not been well explored. Indeed, the effluent wastewater from the tanneries and textile factories is a complicated combination, and unmodified membranes are unable to effectively treat and remove dyes. Therefore, an appropriate technique for modernizing a PES membrane with GO for the elimination of AB-210 is needful.

Additionally, the impact of embedding the PES/GO solution on the cross-sectional configuration of a membrane has never been fully explored. In the present study, GO particles were added to PES casting solutions for the separation of dye from the wastewater produced by tanneries and textile industries. The influence of GO on cross-sectional geometry and hydrophilicity was studied extensively. The permeation flow and ionic species sorption capacity of AB-210 were used to evaluate the efficiency of PES membranes.

EXPERIMENTAL WORK

Chemical materials

In this study, chemical reagents were used for the purpose of preparing polymers, nanomaterials, as well as membranes. These materials are qualitatively controlled materials and were used according to standard specifications (Kadhim et al. 2020).

Graphene oxide preparation

A modified Hummers process was used to make graphene oxide (GO). To begin, a solution that included 120 cm^3 concentrated H_2SO_4, 15.6 g $K_2S_2O_8$, and 16.8 g P_2O_5 was prepared. Secondly, 30 g of graphite was added to the solution which was reflowed at 75–80 °C for four hours. Next, the prepared solution was allowed to cool at room temperature. The solution was then filtered and rinsed with distilled water until the pH was equal to 7. An oven was used to dry the product at 60 °C for 48 h (Kadhim et al. 2020, Sadiq et al. 2020).

The membrane preparation

To prepare the membrane even with coding (1–7), the PES powder (21% wt.) was dissolved in dimethyl sulfoxide (DMSO) solvent (79% wt.) and agitated for 24 hours at ambient temperature using a magnetic stirrer. The GO weight content ratios were 0%, 0.1%, 0.2%, 0.3%, 0.5%, 1.5%, and 2%. The PES/GO mixed solution was then placed in an ultrasonic water bath (50–100 watts/gallon) for 30 minutes to prevent GO-NP aggregation in the last pouring out of the solution. The pouring out of the solution was then placed onto a pre-cleared glass sheet, and the casting was performed at normal lab temperature using a self-made casting knife by moistening the pouring solution in water (Kadhim, Al-Ani et al. 2020). By immersing the pouring solution in a mixed water coagulation container for a period of 24 hours, the phase inversion was achieved. The membrane was then removed from the bath and properly cleaned with dual deionized water (DDI) before being kept in new DDI. To prevent the membrane structure from collapsing, the membrane was then immersed in another water bath containing glycerin.

Experimental work of the membrane filtration

By using the section-flow infiltration technique described in Figure 1, the pure water flow (PWF) of the authentic and PES/GO mixed membrane was determined. The membrane liquidation surface area was equal to 16 cm^2. Each membrane sample was first pre-compacted for a period of not less than 90 minutes or till the flux reached 3 bar. Then, at a constant pressure of 3 bar and a temperature of 25±1 °C, filtration tests were performed. Four aqueous solutions of Acid Black-210 were used in the rejection test. The pH of the AB-210 dye solution was set at 5. The concentration of dye in the permeate solution was evaluated using a spectrophotometer (UV 1100) at 460 nm to estimate the segregation efficiency of the membranes. Equations (1) and (2) were used to calculate the produced pure water flow, f ($L/m^2 \cdot h$), and dye segregation efficiency (R%), respectively (Kadhim et al. 2021):

$$f = \frac{V'}{A_s . t_i} \tag{1}$$

where: f – the pure water flow permeation through the membrane ($L\ m^{-2}h^{-1}$);
V' – the permeate collected volume (L);
t_i – the permeate collected time (h);
A_S – surface area of the membrane (m^2).

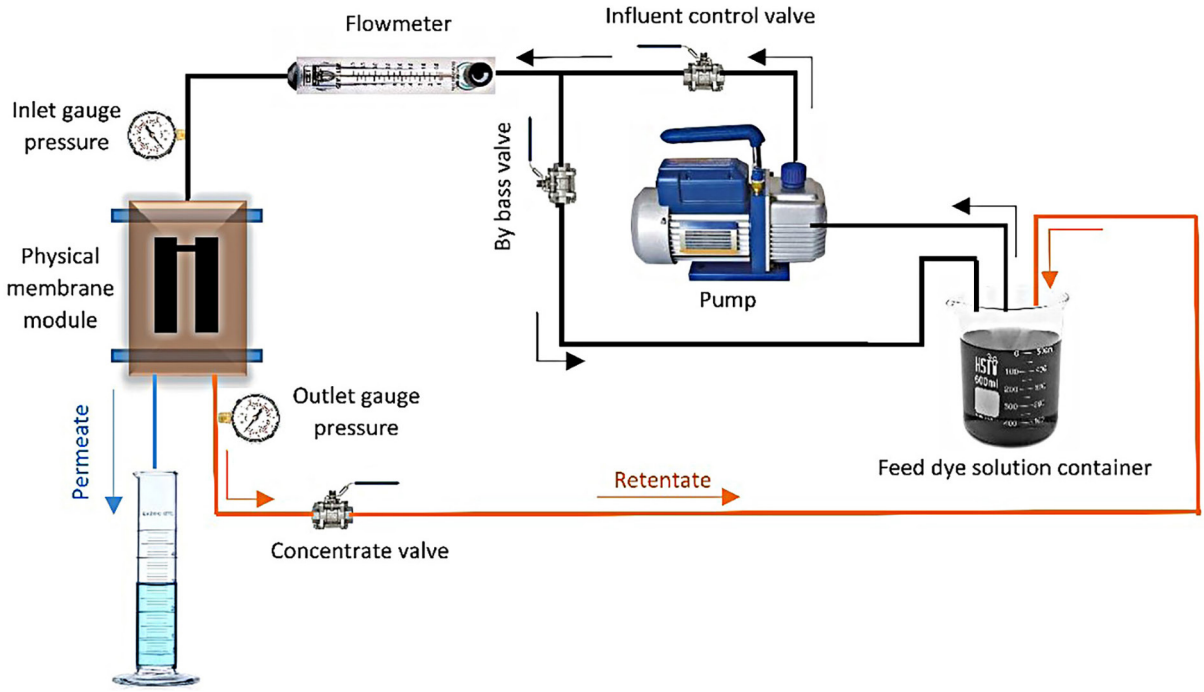

Figure 1. The flow diagram for the membrane filtration system

$$R\% = \left(1 - \frac{C_f}{C_p}\right) \times 100 \quad (2)$$

where: C_f and C_p – the dye concentration in the feeding solution, and the penetrate water (mg/ℓ), respectively.

RESULTS AND DISCUSSION

The composite membranes characterization

Morphology analysis with scanning electron microscopy

The sections of the membranes, whether synthetic PES or those used in control were examined by taking the pictures showing the section of the membranes for different ratios of GO. The symmetrical, porous structure of all synthetic PES membranes was observed, with the configuration consisting of duel layers. An extensive layer with a long and slim finger-like shape emerged towards the upper edge of the membrane. A thin layer with a sponge-like assembly and several semi-elliptical cavities emerged towards the border of the bottom surface. The narrow finger-like shape eventually changed into a broad finger-like shape, reaching the edge at the bottom face when the GO was immersed in the casting solution at various concentrations. This examination shows the phases of influence of different GO quantities embedded in the polymeric solution on the cross-sectional configuration of combined membranes.

The creation of larger holes is due to the fact that GO, as a hydrophilic midst, speeds up the exchange flow rate between the solvent (DMSO) and nonsolvent (water as the coagulation media) during the mode reversal process (Vatanpour et al. 2011). The migration of GO to the membrane surface would increase the membrane hydrophilicity due to the presence of hydrophilic functional groups (Zinadini et al. 2014). The surface of the membrane was relatively smooth, and no holes were found in any of the produced membranes.

This outcome is consistent with our hypothesis that adding GO to the PES pouring solution will speed up the interchange rate between DMSO/water during budding membrane development at high-level polymer concentrations. As a result, a selective layer with smooth skin developed (Ismael 2017). EDX analysis was used to verify the elemental composition of the control and modified nanocomposite PES membranes. The diffusion of GO-NP (i.e., carbon element) in the membrane was enhanced by adding diverse amounts of GO-NP to the pouring mixed solution. Most notably, the C in the membrane matrix agglomerated more when the GO-NP was loaded into the PES polymer casting solution. The excellent dissolution rate of the ultrasonic device and homogenization of the GO in the pouring solution contributed to this.

Mean pore radius and atomic force microscopy

The PES and PES/GO hybrid membranes were measured using a scanning process with a resolution of 8000×8000 nm scanning region of the 3D AFM. The darker portions in these images indicate membrane holes or troughs, whilst the strongest parts reflect the highest nodules on the membrane surface layer. The PES nodules in the control group were large and linked on the 3D-surface layer. Furthermore, adding 0.1 wt.% of GO to the PES pouring solution increased the number of nodules. This process shows that when the GO concentration in the casting liquid solution grew to 0.5 wt.%, the number of nodules increased, but their bulk size at the membrane layer shrank.

The nodules were evenly formed and uniformly dispersed on the membrane surface when the GO concentration was raised from 1.5 wt.% to 2 wt.%. Pore size and distribution are well-indicated by nodule size and density (Al-Ani, Alsalhy et al. 2020). The impact of GO content (wt.%) on the mean surface layer roughness and mean of the pore radius for the top surface layer of control PES and PES/GO membranes are shown in Table 1 (Kadhim et al. 2020). There is no evident pattern in the effect of GO on membrane roughness, as can be shown. Generally, it can be inferred that the addition of GO to the casting solution reduces mean roughness. When the concentration of GO was 0.5 wt%, the mean pore radius of the membrane increased dramatically from a value of 8.25 nm for the control PES to 15.55 nm. The mean pore radius of the composite membranes grew to 15.59 nm when the quantity of GO (1.5 wt%) was raised further, whereas a little reduction was detected as the amount of GO was increased to 2 wt%. The high hydrophilic nature of GO for water enhanced the interchange rate between the DMSO/water (e.g., immediate liquid solution/liquid solution demixing process) (Mahmoodi et al. 2017).

PROCESS OF MODELING AND OPTIMIZATION

Membrane technology frequently causes the issues with energy efficiency. As a result, the central purpose of the optimization and modeling processes is to reduce energy consumption while retaining high permeance during operation. The goal of this project was to improve the operating situations for using GO-NP flat sheet membranes in NF processes. The impact of variables like pH (3–11), added GO-NP (0–2.0 wt.%) in the pouring solution, and dye concentration (10–100 ppm) on the PES membrane permeability for each of the analyzed dyes, AB-210, was investigated. The most successful NF procedure will generate an appropriate value of permeability if the optimal operating variables are determined.

Optimization of operating parameters

Using the NF membrane technique, a series of tests were carried out, each modifying one factor with time to determine the necessary set of operational factors while keeping the other factors steady. The purpose of the optimization process is to ascertain the effect of independent variables, such as pH, AB-210 dye concentration, and GO-NP weight content, on the flow of the permeate mechanism. MINITAB®17 software was used to conduct the analyses. The modified PES/GO flat sheets used in this procedure have a 39.21° interaction angle underneath 3-bar pressure due to their improved membrane performance. Using the ANOVA technique, the stated feature for membrane permeability sensitivity was statistically confirmed. Using the same technique, the stated feature for membrane permeability sensitivity was statistically confirmed, which yielded excellent coefficient values for the AB-210 dye, $R^2 = 0.7069$. Table 2 demonstrates the experimental values and symbols of the parameters.

Table 1. Roughness and Mean pore size for the top surface of the blend membranes

GO wt.% in PES membrane	Mean roughness (nm)	Top surface mean pore radius (nm)
0	45.5	8.25
0.1	36	5.29
0.2	111	11.55
0.3	77.1	14.06
0.5	22	14.59
1.5	41	15.59
2.0	28.9	15.55

Table 2. Values and symbols of the experimental variables at different levels

Parameters	Symbol	Units of measurement	Lower limit	Higher limit
GO-NP	X1	wt. of content %	0	2
AB 210 dye concentration	X2	ppm	10	100
pH of dye solution	X3	unitless	3	11
Permeability	Y	LMH/bar	Target	

Random distribution was employed to eliminate any progressive errors in the layout for optimization, making it easier to find the best values of the operational elements for NF process.

ANOVA statistical modeling

ANOVA is a statistical model used to assess the fluctuations between various parameters in a regression analysis; more specifically, this method is used to explain the influence of independent factors on dependent variables. By assessing the relative significance of the variables, ANOVA may be used to more precisely select the best set of operating parameters. MINITAB®17 was used to perform ANOVA calculations, with a threshold of the relevance of 5% required to examine a variable critical to the process of execution. Table 3 shows the ANOVA outcomes for permeation as a consequence of GO-NP weight ratios, dye concentrations, and pH values, where each one of the independent variables in the layout of design has a *p*-value in the ANOVA table. The differences are statistically significant when the *p*-value is less than 5% (Eleiwi and Laleg-Kirati, 2014).

The ANOVA for membrane flux rate. Response Surface Regression: J versus X_1, X_2, X_3, AB-210 Concentration, Table 3. Regression Equation in Uncoded Units of AB-210 Concentration (Equation 3):

$$Y = 38.2 - 5.73X_3 + 0.212X_2 + 198.3X_1 + \\ + 0.368(X_3)^2 - 0.00184(X_2)^2 - 92.1(X_1)^2 - \\ - 0.0233X_3X_2 - 0.104X_2X_1 \quad (3)$$

Table 4 displays the ANOVA for membrane permeability and response surface regression for the AB-210 dye.

Table 5 presents the predicted response of the membrane flux rate.

Table 3. Variance Analysis using ANOVA for the permeability of the AB-210 dye

Source	DF	Adj SS	Adj MS	*f*-value	*p*-value
Model	8	36845.4	4605.7	11.76	0.000
Linear	3	3563.8	1187.9	3.03	0.041
pH	1	624.2	624.2	1.59	0.214
Concentration	1	1912.6	1912.6	4.88	0.033
% GO	1	1025.1	1025.1	2.62	0.114
Square	3	33282.8	11094.3	28.33	0.000
pH × pH	1	134.1	134.1	0.34	0.562
Conc. × conc.	1	124.1	124.1	0.32	0.577
%GO × %GO	1	30536.8	30536.8	77.96	0.000
2-way interaction	2	293.1	146.6	0.37	0.690
pH × Conc.	1	128.8	128.8	0.33	0.570
Conc. × %GO	1	183.4	183.4	0.47	0.498
Error	39	15275.4	391.7		
Lack-of-fit	35	15275.4	436.4	349152.05	0.000
Pure error	4	0.0	0.0		
Total	47	52120.8			

S	R-sq	R-sq(adj)	R-sq(pred)
19.7908	70.69%	64.68%	50.66%

DF: degrees of the freedom; Adj SS: adjusted summation of squares; Adj MS: adjusted summation of mean squares; F: variability measure of the sample; P: contribution percentage.

Table 4. ANOVA results for membrane flux rate. Response Surface Regression: J versus X_1, X_2, X_3

Coded coefficients					
Term	Coef	SE coef	*t*-value	*p*-value	VIF
Constant	113.75	8.55	13.30	0.000	
pH	-7.44	5.89	-1.26	0.214	1.14
Conc.	-11.61	5.26	-2.21	0.033	1.92
GO%	8.46	5.23	1.62	0.114	1.03
pH × pH	5.9	10.1	0.59	0.562	1.10
Conc. × conc.	-3.73	6.62	-0.56	0.577	1.00
GO% × GO%	-92.1	10.4	-8.83	0.000	1.16
pH × conc.	-4.20	7.32	-0.57	0.570	1.34
Conc. × GO%	-4.69	6.85	-0.68	0.498	1.57
Fits and diagnostics for unusual observations					
Obs	Flux	Fit	Resid	Std resid	
26	65.40	108.28	-42.88	-2.57	R
27	66.50	45.81	20.69	1.59	
33	55.80	101.42	-45.62	-2.50	R
40	49.90	92.41	-42.51	-2.31	R
47	40.20	84.57	-44.37	-2.56	R

Table 5. Predicted response of the membrane flux rate

Response optimization: flux ($L \cdot m^{-2} \cdot hr^{-1}$)						
Parameters						
Response	Goal	Lower	Target	Upper	Weight	Importance
flux	Maximum	5.7	110		1	1
Solution						
Solution	pH	Concentration	% GO	Flux fit	Composite desirability	
1	3	10	0.5	131.234	1	
Multiple Response Prediction						
Variable			Setting			
pH			3			
Concentration			10			
% GO			0.5			
Response	Fit	SE Fit	95% CI	95% PI		
Flux	131.2	13	(104.9; 157.6)	(83.3; 179.2)		

RESULTS ANALYSIS AND EVALUATION

Effect of pareto chart and main effects of the plot

Figure 2 shows a Pareto chart of the standardized effects for dye permeability. The figure shows how the main factors, such as pH (which is factor A), dye feed amount per unit volume (factor B), added GO-NP weight percent (factor C), and lot interaction causes, affect dye permeability. As a result, to be consistently meaningful at the 5% level, regular effect value of every coefficient must be greater than the critical value of 2.023. The term (CC), which reflects the quadratic impact, demonstrates the significance of the GO wt.% content. The GO wt.% content has the most significant standardized impact (factor C). Factors B and C are both above the critical value, as illustrated in Figure 2. (i.e., they were significant). Regardless, the feed pH (factor A) had a slight and insignificant influence.

The primary impact plot for the dye permeability is shown in Figure 3. The GO wt.% percent was the majority remarkable factor, followed by dye concentration and pH, according to the layout

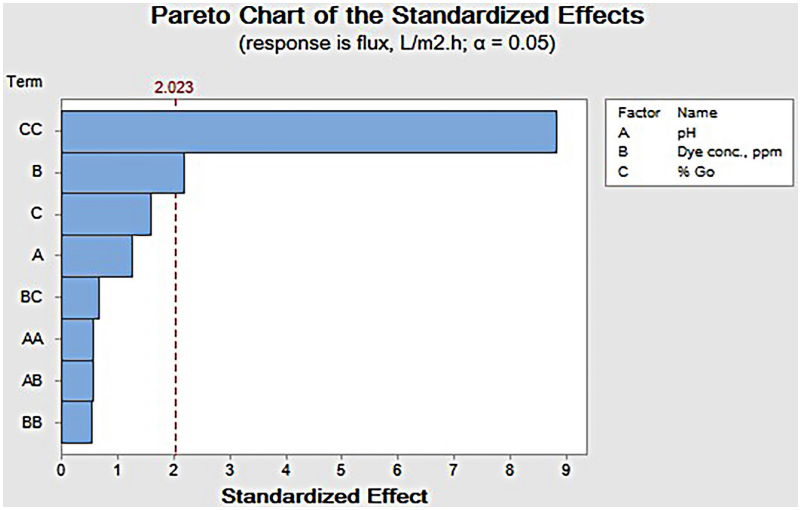

Figure 2. Pareto chart of the standardized impact of factors on the permeability of AB-210: pH (A), concentration (B), and GO wt.% (C)

a)

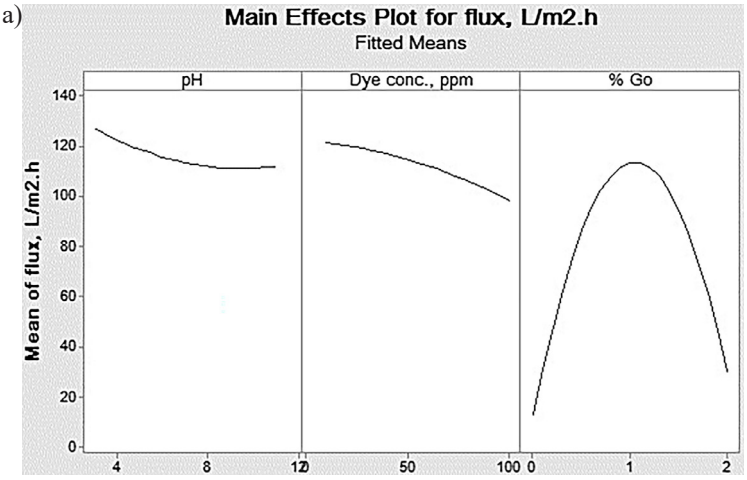

b)

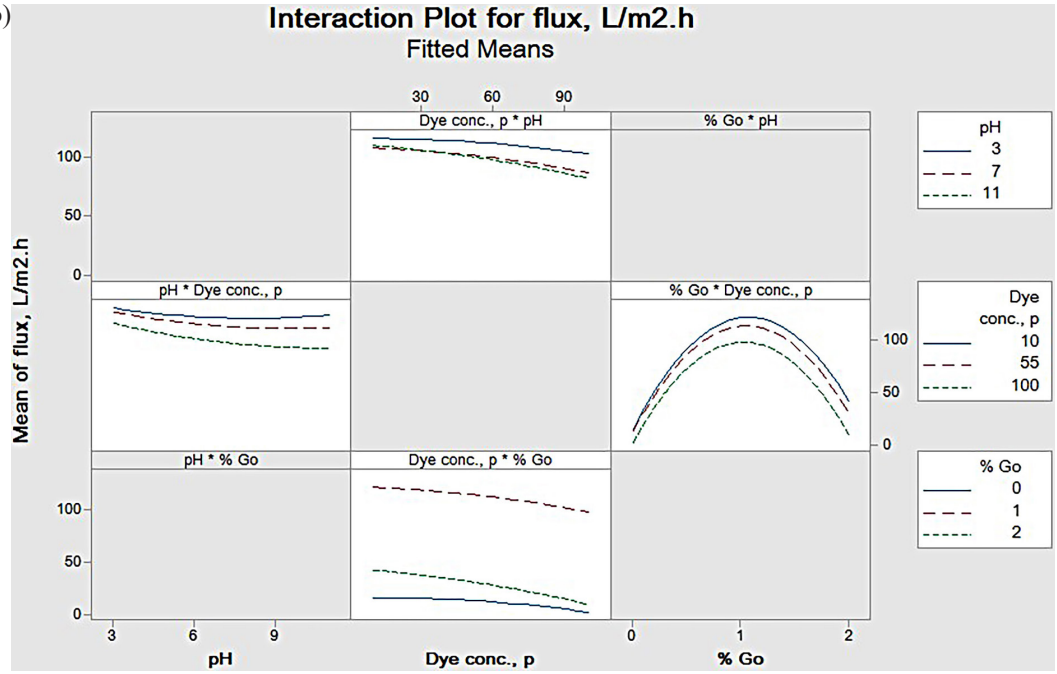

Figure 3. (a) Primary influence track of pH value, dye concentration, and GO wt.% on the permeability of AB-210 dye, (b) The interaction plot for flux

of primary impacts. The permeability increased as the GO wt.% content grew to a reasonable level of about 1.0 wt.%, then reduced at 2.0 wt.% of GO. As shown in Figure 3a, permeation grew as the loading rate concentration was changed from high to low (i.e., from 100 to 10 ppm). The pH of the AB-210 dye solution had essentially little effect on permeability, as seen in Figure 3a, and the pH level may be anywhere between 3 and 11. Figure 3b illustrates the variables-flux interaction so that the main flux can be calculated through any point of the variables.

Residuals in a normal probability plot

A natural probability chart is a visual tool for detecting if a reported data set is naturally distributed. In contrast to a theoretical normal distribution, data is depicted in a modal where the points might be placed along a straight line. The points which are not on a straight line should be discarded since their values are invalid. All data residuals are typically scattered in the displayed results such that the total points form an essentially straight line, as seen in Figure 4.

Residuals vs. order and fits plot

The fitness of ANOVA results is measured using a residual graph. The residuals vs. the independent parameters are shown in Figures 5a and 5b. The best method to produce an independent error is to arrange the randomization of experimental trials according to two basic possibilities regarding errors; errors are independent of one another and the best approach to generate an independent error is to plan the randomization of experiments conducted. Furthermore, the error disparity is unaffected by the variability degrees of the parameters or by the projected response values.

Analysis of the response surface

The response of dye permeability is shown as a 3D contact surface space, with the permeability placed against the boundaries of two variables. The major goal of the response surface graph is to find the ideal operating parameters for maximal permeability, which are represented by pH, GO wt.% ratio, and AB-210 dye concentration. The fitted model was used to create 3D responding surface graphs and 2D response contour plots, as illustrated in Figure 6.

The AB-210 dye permeability function response to the surface 3D graph and contour graph (Figure 6A, 6C) demonstrated that reducing pH and shrinking the feed concentration resulted in increased permeability at a constant GO wt.% (i.e., 1.0 wt.%). Nevertheless, as anticipated, for lesser concentrations, the impact of changing pH on permeability was not significant. When the third component (pH) was kept constant at 5, the influence of the two parameters, GO wt.% and concentration is seen in Figures 6B and 6D.

The permeability rose to more than 120 LMH/bar when the GO wt.% was raised to 1.0, whereas altering the concentration had no effect on the permeability. The tendency was reversed for larger GO content ratios (GO content > 1.0 wt.%). The

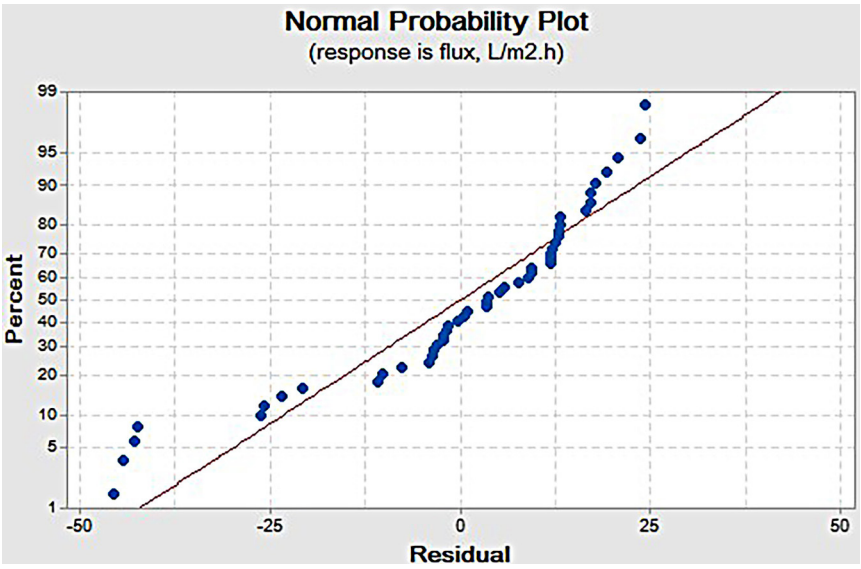

Figure 4. Normal probability sketch of the residuals for AB-210 permeability

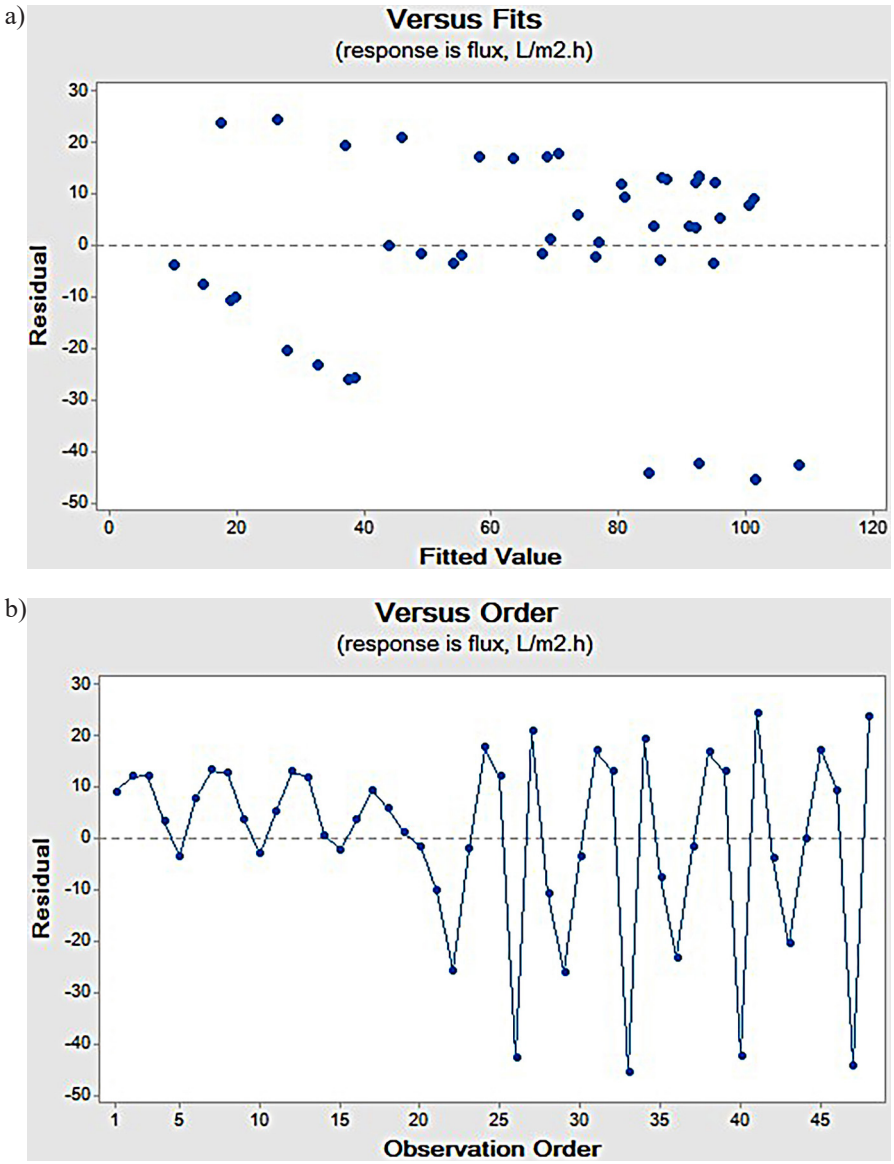

Figures 5. a) Residuals vs. b) the observation orders and fitted values gragh of AB-210 permeability

permeability response also revealed that the attraction impact between the GO weight ratio and concentration was reduced.

Optimization of the NF membrane permeability

Figure 7 depicts the membrane permeability optimization design with varying amounts of the three parameters. The data from the MINITAB®17 was used to construct the optimization chart. The optimization outputs are featured on the left axis, with the best value for every parameter depicted in the top row, which is shown in red color. The best operating parameters for the AB-210 dye solution, according to Figure 7, are a feed pH value of 3, a dye concentration of 10 ppm, and 1.0707 GO wt.%, while 131.233 $L \cdot m^{-2} \cdot h^{-1} \cdot bar^{-1}$ is believed to be the maximum permeability. The key component in this operation was the addition of GO weight ratios to the pouring solution; after that, the secondary influence of dye concentrations was affected.

The existence of a horizontal axis indicates that the input pH levels had no meaningful impact on the permeability of the membrane. The primary component in this procedure, as with the AB-210 dye, was the additional GO weight percent in the pouring solution, followed by the dye concentrations as a minor influence. When a line deviates slightly from the horizontal, as the pH line does, the reaction might be affected. The lower steep incline of the line demonstrates that the pH value had lesser influence

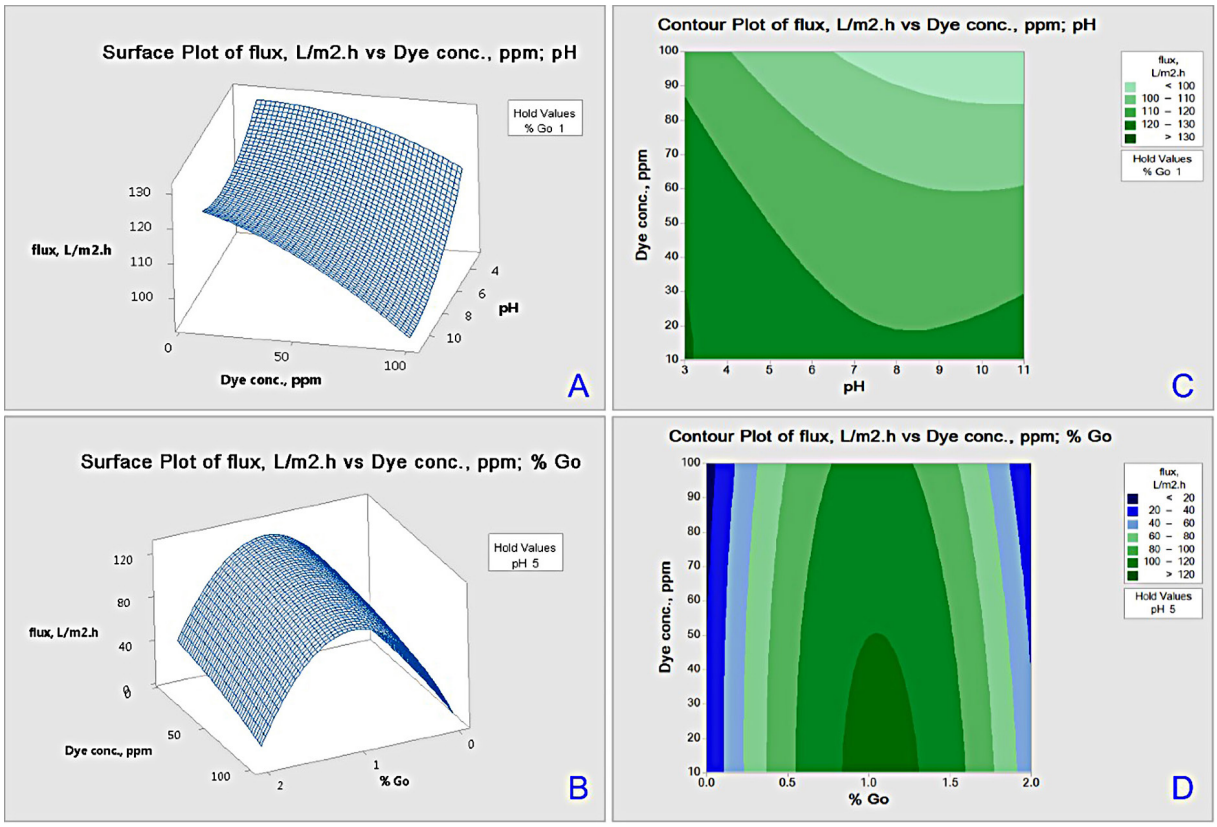

Figure 6. 3D response surface plot (A, B), and 2D contour gragh of response (C, D) of the permeability as a function of the GO wt.%, pH, and AB-210 dye concentration

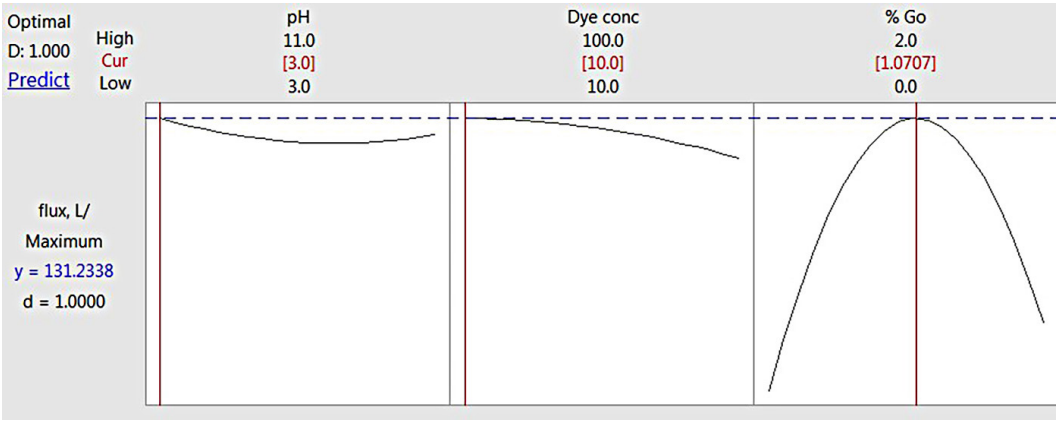

Figure 7. Optimization plot of the process parameters for the maximum permeability for AB-210

on permeability than the other components. As can be observed in Figure 6, utilizing produced membranes with varying concentrations of GO at varied solution concentrations tends to increase dye solution permeability.

The increased hydrophilicity and surface morphology of the generated membranes with the addition of GO wt.% might explain the greater permeate of the fabricated membranes. High hydrophilicity and porosity membranes have the best permeability. When the primary concentration for the AB-210 was increased, it resulted in a relative reduction in permeability. This drop has been documented in the literature as a result of dye molecule adsorption on the surface of the membrane, which causes a cake layer to develop on the membrane surface, preventing water from passing through and lowering flow (Yahya, Rashid et al. 2021). The acidity of the dye, on the other hand, had minimal impact on the permeability of the AB-210 dye, with no discernible effect.

CONCLUSIONS

The plain sheet of the PES-NF membranes was modified with the GO-NP material for dye removal. GO was impregnated into the PES polymeric matrix at various feeding ratios (i.e., 0, 0.1, 0.2, 0.3, 0.5, 1.5, and 2.0 wt.%) using the conventional non-solvent induced phase separation (NIPS) approach. Using one AB-210 dye model, the penetration and separation properties of all control and plain membranes were extensively reported. The running parameters that have the greatest influence on the permeability of the PES/GO thin sheet membranes in the NF process were determined using optimization procedures. The GO wt.%, AB-210 dye concentration, and pH were discussed as three criteria that had the greatest impact on permeance. The experimental design enabled us to look at the effects of three different dye levels.

The permeability was primarily influenced by the GO content and dye concentration in these studies. The permeability of the AB-210 dye, on the other hand, was unaffected by its input pH. On the basis of multiple studies, the design also allowed for the specification of the best values for the three elements. For the dye investigated, the best parameters were GO (almost 1.0 wt.%) and feed dye concentration (10 ppm), with a pH range of 3–11. The higher permeability attained under these circumstances was 131.2338 $L \cdot m^{-2} \cdot h^{-1} \cdot bar^{-1}$.

REFERENCES

1. Abdel-Karim, A., Sebastian, L., Monica, A., Aravind, V., Xiaolei, F., Stuart, H.M., Eglal, S.R., Mohamed B.I., Patricia G. 2018. High flux and fouling resistant flat sheet polyethersulfone membranes incorporated with graphene oxide for ultrafiltration applications. Chemical Engineering Journal, 334, 789–799.
2. Akbari, M., Shariaty-Niassar M., Matsuura T., Ismail A.F. 2018. Janus graphene oxide nanosheet: A promising additive for enhancement of polymeric membranes performance prepared via phase inversion. J Colloid Interface Sci, 527, 10–24.
3. Al-Ani, F.H., Alsalhy, Q.F., Raheem, R.S., Rashid, K.T., Figoli, A. 2020. Experimental Investigation of the Effect of Implanting TiO2-NPs on PVC for Long-Term UF Membrane Performance to Treat Refinery Wastewater. Membranes (Basel), 10(4.
4. Al-Sultan, A.A., Al-Wakel, S.F., Al-Taie, A.S. 2019. Experimental Study of Heavy Metal Dispersion through Cohesionless Soil: a Case Study of Cd+. International Review of Civil Engineering, 16(6).
5. Alsalhy, Q.F.,. Ibrahim, S.S., Khaleel, S.R. 2017. Performance of vacuum poly(propylene) membrane distillation (VMD) for saline water desalination. Chemical Engineering and Processing - Process Intensification, 120, 68–80.
6. Alyarnezhad, S., Marino, T., Parsa, J.B., Galiano F., Ursino C., Garcia H., Puche M., Figoli A. 2020. Polyvinylidene Fluoride-Graphene Oxide Membranes for Dye Removal under Visible Light Irradiation. Polymers (Basel), 12(7).
7. De Gisi, S., Lofrano G., Grassi M., Notarnicola M. 2016. Characteristics and adsorption capacities of low-cost sorbents for wastewater treatment: A review. Sustainable Materials and Technologies, 9, 10–40.
8. Eleiwi, F., Laleg-Kirati, T.M. 2014. Dynamic modeling and optimization in membrane distillation system. 19th World Congress The International Federation of Automatic Control Cape Town, South Africa. August, 24–29.
9. Fauzi, I.A., Matsuura, T. 2016. Membrane Technology for Water and Wastewater Treatment, Energy and Environmentby London, UK, CRC Press, Taylor & Francis Group.
10. Geim, A.K. 2009. Graphene: Status and Prospects. Science, 324.
11. Geim, A.K., Novoselov, K.S. 2007. The rise of graphene. Nature Materials, 6.
12. Gerken, M., Moran, M.D., Mercier, H.P., Pointner, B.E., Schrobilgen, G.J., Hoge, B., Christe, K.O., Boatz, J.A. 2009. On the XeF+/H2O System: Synthesis and Characterization of the Xenon (II) Oxide Fluoride Cation, FXeOXeFXeF+. Journal of the American Chemical Society, 131.
13. Gholami, N., Mahdavi, H. 2018. Nanofiltration composite membranes of polyethersulfone and graphene oxide and sulfonated graphene oxide. Advance in Polymer Technology, 37. (8)
14. Ismael, A.E. 2017. Nano Submerged Membrane Bioreactor for Hospital Wastewater Treatment, University of Technology.
15. Jin, F., Lv W., C. Zhang, Z. Li, R. Su, W. Qi, Q. Yang and Z. He (2013). High-performance ultrafiltration membranes based on polyethersulfone–graphene oxide composites. RSC Advances, 3(44)
16. Judd, S., Judd, C. 2011. Principles and Applications of Membrane Bioreactors for Water and Wastewater Treatment, Elsevier.
17. Junaidi, N.F.D., Khalil N.A., Jahari A.F., Shaari N.Z.K., Shahruddin M.Z., Alias N.H., Othman N.H. 2018. Effect of Graphene Oxide (GO) on the Surface Morphology & Hydrophilicity of Polyethersulfone (PES). IOP Conference Series: Materials Science and Engineering, 358.

18. Kadhim, R.J., Al-Ani, F.H., Al-Shaeli, M., Alsalhy, Q.F., Figoli A. 2020. Removal of Dyes Using Graphene Oxide (GO) Mixed Matrix Membranes. Membranes (Basel), 10(12)
19. Kadhim R.J., Al-Ani F.H., Alsalhy Q.F., Figoli A. 2021. Optimization of MCM-41 Mesoporous Material Mixed Matrix Polyethersulfone Membrane for Dye Removal. Membranes (Basel), 11(6)
20. Koyuncu, I. 2002. Reactive dye removal in dye/salt mixtures by nanofiltration membranes containing vinylsulphone dyes: Effects of feed concentration and cross flow velocity. Desalination, 143, 243–253.
21. Kumar, M., McGlade, D., Ulbricht, M., Lawler, J. 2015. Quaternized polysulfone and graphene oxide nanosheet derived low fouling novel positively charged hybrid ultrafiltration membranes for protein separation. RSC Advances, 5(63), 51208–51219.
22. Lin, J., Ye, W., Baltaru, M.C., Tang, Y.P., Bernstein, N.J., Gao, P., Balta, S., Vlad, M., Volodin, A., Sotto, A., Luis, P., Zydney, A.L., Van der Bruggen, B. 2016. Tight ultrafiltration membranes for enhanced separation of dyes and Na2SO4 during textile wastewater treatment. Journal of Membrane Science, 514, 217–228.
23. Luque-Alled, J., Abdel-Karim A., Alberto, M.A,. Sebastian L., Maria, P., Kun, H., Aravind, V., El-Kalliny, A.S., Holmes, S.M., Patricia, G. 2020. Polyethersulfone membranes: From ultrafiltration to nanofiltration via the incorporation of APTS functionalized-graphene oxide. Separation and Purification Technology, 230.
24. Mahmoodi, N.M., Ghezelbash, M., Shabanian, M., Aryanasab, F., Saeb, M.R. 2017. Efficient removal of cationic dyes from colored wastewaters by dithiocarbamate-functionalized graphene oxide nanosheets: From synthesis to detailed kinetics studies. Journal of the Taiwan Institute of Chemical Engineers, 81, 239–246.
25. Mahmoud, K.A., Mansoor, B., Mansour, A., Khraisheh M. 2015. Functional graphene nanosheets: The next generation membranes for water desalination. Desalination, 356, 208-225.
26. Majewska-Nowak, K. 2009. Ultrafiltration of Dye Solutions in the Presence of Cationic and Anionic Surfactants. Environment Protection Engineering, 35.
27. Makhetha, T.A., Moutloali, R.M. 2018. Antifouling properties of Cu(tpa)@GO/PES composite membranes and selective dye rejection. Journal of Membrane Science, 554, 195–210.
28. Moussavi, G., Mahmoudi, M. 2009. Removal of azo and anthraquinone reactive dyes from industrial wastewaters using MgO nanoparticles. Journal of Hazardous Materials, 168(2–3): 806-812.
29. Obiad, A.J., Al-Sultan, A.A. 2020. CWWQI on the Evaluation of Effluent Wastewater from Al-Dora Refinery WWTP. IOP Conference Series: Materials Science and Engineering.
30. Park, H., Chang, I., Lee, K. 2015. Principles of Membrane Bioreactors for Wastewater Treatment, CRC Press, Taylor & Francis Group.
31. Pendergast, M.M., Hoek E.M.V. 2011. A review of water treatment membrane nanotechnologies. Energy & Environmental Science, 4(6)
32. Sadiq, A.J., Shabeeb, K.M., Khalil, B.I., Alsalhy, Q.F. 2020. Effect of embedding MWCNT-g-GO with PVC on the performance of PVC membranes for oily wastewater treatment. Chemical Engineering Communications, 207(6)
33. Sarbatly, R. 2020. Membrane Technology for Water and Wastewater Treatment in Rural Regions. Hershey PA, USA, IGI Global.
34. Van der Bruggen, B., Daems, B., Wilms, D., Vandecasteele, C. 2001. Mechanisms of retention and flux decline for the nanofiltration of dye baths from the textile industry. Separation and Purification Technology, 22, 519–528.
35. Vatanpour, V., Madaeni S.S., Moradian R., Zinadini S., Astinchap B. 2011. Fabrication and characterization of novel antifouling nanofiltration membrane prepared from oxidized multiwalled carbon nanotube/polyethersulfone nanocomposite. Journal of Membrane Science, 375(1–2), 284–294.
36. Wang, X., Feng, M., Liu, Y., Deng, H., Lu, J. 2019. Fabrication of graphene oxide blended polyethersulfone membranes via phase inversion assisted by electric field for improved separation and antifouling performance. Journal of Membrane Science, 577, 41–50.
37. Yahya, A. A., K. T. Rashid, M. Y. Ghadhban, N. E. Mousa, H. S. Majdi, I. K. Salih and Q. F. Alsalhy (2021). "Removal of 4-Nitrophenol from Aqueous Solution by Using Polyphenylsulfone-Based Blend Membranes: Characterization and Performance." Membranes (Basel) 11(3).
38. Yaseen, D. A. and M. Scholz (2018). "Textile dye wastewater characteristics and constituents of synthetic effluents: a critical review." International Journal of Environmental Science and Technology 16(2): 1193–1226.
39. Zhao, C., X. Xu, J. Chen, G. Wang and F. Yang (2014). "Highly effective antifouling performance of PVDF/graphene oxide composite membrane in membrane bioreactor (MBR) system." Desalination 340: 59–66.
40. Zinadini, S., A. A. Zinatizadeh, M. Rahimi, V. Vatanpour and H. Zangeneh (2014). "Preparation of a novel antifouling mixed matrix PES membrane by embedding graphene oxide nanoplates." Journal of Membrane Science 453: 292–301.